

Supplementary Material

Systemic siRNA Delivery With a Dual pH-Responsive and Tumor-targeted Nanovector for Inhibiting Tumor Growth and Spontaneous Metastasis in Orthotopic Murine Model of Breast Carcinoma

Bo Fan^{a,c}, Lin Kang^a, Liqing Chen^a, Ping Sun^a, Mingji Jin^a, Qiming Wang^a, You Han Bae^b, Wei Huang^{a,*}, Zhonggao Gao^{a,*}

^a State Key Laboratory of Bioactive Substance and Function of Natural Medicines, Department of Pharmaceutics, Institute of Materia Medica, Chinese Academy of Medical Sciences and Peking Union Medical College, Beijing 100050, PR China

^b Department of Pharmaceutics and Pharmaceutical Chemistry, College of Pharmacy, University of Utah, Rm 2972, Skaggs Pharmacy Institute, 30S 2000E, Salt Lake City, Utah 84112, USA

^c School of Pharmaceutical Science, Shanxi Medical University, No. 56, Xinjian Nan Road, Taiyuan 030001, Shanxi, People's Republic of China.

* Corresponding authors: Zhonggao Gao and Wei Huang, E-mails: zggao@imm.ac.cn (Z. Gao) and huangwei@imm.ac.cn (W. Huang), Tel.: +86 10 63028096.

1. Materials

Branched polyethyleneimine with the MW of 1,800 (PEI1.8k) and 3-(3,4-dihydroxyphenyl) propionic acid (DHPA) were purchased from Alfa Aesar Ltd. (Tianjin, China). α -methoxy ω -amino poly(ethylene glycol) amine (mPEG-NH₂, MW 2kDa) was purchased from JenKem Technology Co. Ltd. (Beijing, China). 2-(bromomethyl) phenylboronic acid (2-Br-PBA) was purchased from Aladdin Industrial Inc. (Shanghai, China). N,N-Diisopropylethylamine (DIEA), Alizarin Red S (ARS) was bought from J&K Chemical Ltd. (Beijing, China). N-(3-Dimethylaminopropyl)-N'-ethylcarbodiimide hydrochloride (EDC), N-hydroxysuccinimide (NHS), 3-(4,5-dimethyl-2-thiazolyl)-2,5-diphenyl-2-H-tetrazolium bromide (MTT) was obtained from Sigma-Aldrich Inc. (Shanghai, China). Fluorescein isothiocyanate labeled sambucus nigra lectin (FITC-SNA), fluorescein isothiocyanate labeled wheat germ agglutinin (FITC-WGA) and fluorescein isothiocyanate labeled maackla amurensis lectin (FITC-MAA) were supplied from Vector Laboratories (Burlingame, CA, USA). Sialidase was purchased from New England Biolabs, Inc. (Hitchin, UK).

2. Synthesis and characterization of the polymers

2.1. Synthesis of mPEG-catechol (mPEG-Cat)

mPEG-Cat was synthesized by coupling between mPEG-NH₂ (MW 2 kDa) and DHPA (**Figure S1A**). DHPA (182.2mg, 1.0mmol) dissolved in 5ml DMF was activated with EDC (383.4mg, 2mmol) and NHS (230.2mg, 2mmol) for 2 h, and then added dropwise to mPEG-NH₂ (1g, 0.5mmol) in 5 ml DMF with DIEA (262 μ l, 1.5mmol). The reaction solution was stirred for 24 hrs at room temperature. Then, the mixture was transferred into a dialysis tube (MWCO 1,000) and dialyzed against deionized water for 48 hrs, followed by lyophilized to obtain white product. The conjugation of DHPA to mPEG was confirmed by ¹H-NMR spectroscopy in CDCl₃. ¹H NMR (600MHz, CDCl₃, δ): 6.75-6.80 (d, 1H, aromatic), 6.70 (s, 1H, aromatic), 6.55-6.60 (d, 1H, aromatic), 2.80-2.85 (t, 2H, adjacent to aromatic), 2.40-2.45

(t, 2H, -NHCO-CH₂-), 3.50-3.70 (m, -O-CH₂CH₂O-), 3.37(s, 3H, OCH₃). The absorbance of catechol group at 280 nm was measured with a UV-Vis spectrophotometer (Implen GmbH., Germany), and the coupling yield was calculated by determining the catechol group concentration from a standard curve of dopamine hydrochloride in a concentration range of 50–250 mM.

As depicted in **Figure S1B**, the structure of mPEG-Cat was confirmed by the characteristic peaks at 6.5-7.0 ppm (m, 3H, aromatic) of DHPA and 3.55-3.67 ppm (m, -O-CH₂CH₂O-) of PEG backbone, respectively.

2.2. Synthesis of PEI-PBA

PEI-PBA was prepared according to the reference with some modifications[1]. Briefly, 2-(bromomethyl) phenylboronic acid (1.289 g, 6 mmol) and PEI1.8k (0.900 g, 0.5 mmol) were dissolved in methanol and stirred at 70°C for 24 hrs. After reaction, the mixed solution was dropped into 30 mL cold ether to acquire a pale-yellow precipitate. Then the crude product was purified by dialysis (MWCO 1,000 Da) against distilled water for 48 h. The polymers were characterized by ¹H NMR spectroscopy (Varian Mercury-600 MHz spectrometer, Varian Medical Systems, Inc., USA). As presented in **Figure S2B**, the peaks at 7.8-6.8 ppm (m, 3H, aromatic) of PBA and 3.0-2.0 ppm (m, 4H, -NCH₂CH₂N) of PEI were evidence for the successful conjugation. Herein, the modification degree of PBA was based on the integration ratio of resonances at 7.8-6.8 ppm (the benzene proton signals of PBA) and 3.0-2.0 ppm (the ethylene proton signals of PEI) in the ¹H NMR spectra. PBA were grafted on PEI1.8k at various substitution degree (DS) (data not shown), and the optimal DS was selected as 20.1%.

2.3. The formation of PEG-CPB-PEI (PCPP)

PEG-CPB-PEI was prepared by mPEG-Cat and PEI-PBA at 1:2 molar ratios of catechol to PBA. Herein, the borate esters act as a “joint” to spontaneously integrate mPEG-Cat and

PEI-PBA into one entity via the conjugation of PBA and Cat in neutral aqueous medium without any catalysts. A typical procedure was used as follows: mPEG-Cat and PEI-PBA were dissolved in HEPES buffer (pH 7.4) and stirred overnight under nitrogen. The product was dialyzed (MWCO 5,000 Da) against distilled water for 48h. Then, the PEG-CPB-PEI polymer was lyophilized and stored at -20 °C for further use. For convenience, PEG-CPB-PEI was further abbreviated as PCPP in the article.

3. The binding capacity of PEI-PBA with *cis*-diols

To verify the binding capacity of PEI-PBA with *cis*-diols in our system, the apparent pK_a of PEI-PBA was first determined by supervising the decrease of absorbance at 268 nm upon increasing pH according to Wang et al.[2]. The UV absorption variations occurred due to the change of hybridization state of boron, which transformed from the trigonal sp^2 geometry into the tetrahedral sp^3 geometry. As shown in **Figure S4A**, the pK_a value was determined to be 7.18. Because most boronic acids are weak lewis acids with a pK_a of *ca.* 8–9, it usually need to be performed in alkaline solution to form stable borate esters (the pH of medium should be equal or greater than the pK_a)[3]. However, this induced the inconvenient operation and a hazard of disassembly of borate esters in physical conditions. In our design, the strategy of borate formation at pH 7.4 is based on the introduction of an amine in *ortho*-position to the boronic acid, which could form an intramolecular B...N interacton (Wulff-type boronic acids)[4]. As the chemical structure of PEI-PBA illustrated in **Figure S2A**, the introduction of an *ortho* aminomethyl group to boronic acid decreased pK_a of boronic acid (**Figure S4A**), which facilitated higher association constants between PBA and *cis*-diols at neutral pH.

Then Alizarin Red S (ARS) was used to investigated the binding affinities of different diols for PBA[2]. ARS is a catechol-containing dye, which could display dramatic color and fluorescent changes upon binding to boronic acid. A PEI-PBA solution (15 mM) was mixed with the ARS solution (0.75mM) in HEPES buffer at pH 7.4. Then, the fluorescence intensity

of PBA-ARS complex was measured after adding different concentrations of *cis*-diols at pH 7.4 using a fluorescence spectrometer (Fluorolog-Tau-3, ISA Co., Ltd., USA) (λ_{ex} 468 nm, λ_{em} 572nm). As illustrated in **Figure S4B**, the binding of PBA with catechol, ribose or glucose induces the fluorescence quenching of PBA-ARS complex due to competitive association between diols[5]. Furthermore, the binding capacity of PBA-glucose was lower than that of PBA-ribose or PBA-catechol, indicating that the glucose level during blood circulation might have little impact on the stability of the siRNA delivery system after intravenous administration.

4. Cytotoxicity assay

The cell toxicity of PCPP copolymer was examined by MTT assays. 4T1 cells were seeded into a 96-well plate. After 24 h culture, cells were incubated with the polymers of serial concentrations from 10 to 500 $\mu\text{g mL}^{-1}$ for 24 or 48 h. Then the medium was removed and 200 μL fresh RPMI 1640 containing 20 μL MTT solution (5 mg/mL in PBS buffer) was added. After further incubation for another 4 h, the medium was discarded and 150 μL DMSO was added to dissolve the formazan crystals. The absorbance was detected at 570 nm using a Synergy H1m Monochromator-Based Multi-Mode Microplate Reader (BioTek., USA). The cell viability was calculated as Equation (S1). The *in vitro* cytotoxicity of nanoparticles containing 100 nM siN.C. at different N/P ratios was also studied as described above.

$$\text{Equation (S1): cell viability (\%)} = \frac{\text{OD}_{570(\text{sample})}}{\text{OD}_{570(\text{control})}} \times 100$$

Figure S5 showed that the cell viability was above 80% when the concentration of polymer was ranging from 10 to 300 $\mu\text{g mL}^{-1}$, indicating negligible cytotoxicity of the PCPP copolymer during this range. Furthermore, no obvious cytotoxicities of PCPP_{siN.C.} nanoparticles were obtained at different N/P-ratios.

5. *In vitro* gene silencing effects of PCPP_{siLuc} nanoparticles for targeting study

The silencing capacity on luciferase reporter gene in 4T1-Luc cells was investigated after treatment with different formulations. As controls, the naked siLuc, PEI1.8k_{siLuc}, PEI-PBA_{siLuc} and Lipofectamine 2000_{siLuc} complexes were used. The reporter assay results were showed in **Figure S6**. The siLuc dose was first investigated. As we can see in **Figure S6A**, when the 4T1-Luc cells were treated with PCPP_{siLuc} at 50 nM, $25.6 \pm 2.0\%$ reduction of the luciferase expression was obtained. When the siLuc concentration was improved to 100 nM, $53.3 \pm 3.6\%$ reduction was observed. However, as the siLuc concentration increased further from 100 nM to 200 nM, the luciferase expression reduced without statistically significant difference ($P > 0.05$). Hence, 100 nM was served as the fixed concentration in future research.

The result of gene silencing effects with different formulations was shown in **Figure S6B**. As compared with PEI1.8k_{siLuc}, PCPP_{siLuc} displayed much higher gene silencing ability, indicating the enhanced effect is attribute to the interaction of PBA with cells. Interestingly, the gene silencing efficiency in the PCPP_{siLuc} group was almost at the same level as that of PEI-PBA_{siLuc}, which suggested that the detachable PEG modification did not inhibit cellular uptake of nanoparticles by target cells. Compared to the permanent PEGylation[6], the detachable PEGylation of gene carriers might achieve prolonged circulation, advanced targeting capacity and enhanced cellular uptake at the same time.

6. The expression of sialylated antigens on cell surface after treatment with sialidase

In order to verify the hydrolysis effect of sialidase, flow cytometry analysis was performed to detect the binding of FITC-SNA, MAA or WGA to SA on 4T1 cell surfaces. Cells were incubated with sialidase (50 mU mL^{-1}) for overnight prior to addition of PCPP/Cy3-siRNA. Sialidase is an enzyme that can cleave SA epitopes from cells. Then the cells were incubated with FITC-SNA, MAA or WGA (SNA $1 \mu\text{g mL}^{-1}$, MAA $5 \mu\text{g mL}^{-1}$, WGA $5 \mu\text{g mL}^{-1}$) for 30 min, followed by flow cytometry analysis. SNA, MAA and WGA are the

lectins, widely used to determine the sialylation in cancer cells[7, 8]. These three lectins each bind different structural subclasses of sialylated epitopes. MAA could specifically recognize α 2,3-linked sialic acid[9]. SNA primarily binds to α 2,6- linked SA on the terminal galactose and to a lesser degree α 2,3- linkage[10]. WGA has a broader selectivity range with binding in any linkage (α 2,3-, α 2,6- or α 2,8-) to N-acetylneuraminic acid and N-acetyl-D-galactosamine besides N-acetyl-D-glucosamine and its β -1,4 linked oligosaccharides[11, 12].

As represented in **Figure S7**, compared with the control groups (PBS treated groups), sharp decreased fluorescent signals ($P < 0.01$) could be determined at the cell surface after sialidase treatment. This meant declined expression of SA after cells were incubated with sialidase overnight.

References

1. Yang B, Jia H, Wang X, Chen S, Zhang X, Zhuo R, et al. Self-assembled vehicle construction via boronic acid coupling and host-guest interaction for serum-tolerant DNA transport and pH-responsive drug delivery. *Advanced healthcare materials*. 2014; 3: 596-608.
2. Yan J, Springsteen G, Deeter S, Wang B. The relationship among pKa, pH, and binding constants in the interactions between boronic acids and diols—it is not as simple as it appears. *Tetrahedron*. 2004; 60: 11205-9.
3. Mulla HR, Agard NJ, Basu A. 3-Methoxycarbonyl-5-nitrophenyl boronic acid: high affinity diol recognition at neutral pH. *Bioorganic & Medicinal Chemistry Letters*. 2004; 14: 25-7.
4. Li H, Liu Y, Liu J, Liu Z. A Wulff-type boronate for boronate affinity capture of cis-diol compounds at medium acidic pH condition. *Chem Commun (Camb)*. 2011; 47: 8169-71.
5. Springsteen G, Wang B. A detailed examination of boronic acid–diol complexation. *Tetrahedron*. 2002; 58: 5291-300.
6. Kim J, Lee YM, Kim H, Park D, Kim J, Kim WJ. Phenylboronic acid-sugar grafted polymer architecture as a dual stimuli-responsive gene carrier for targeted anti-angiogenic tumor therapy. *Biomaterials*. 2016; 75: 102-11.
7. Bull C, Boltje TJ, van Dinther EA, Peters T, de Graaf AM, Leusen JH, et al. Targeted delivery of a sialic acid-blocking glycomimetic to cancer cells inhibits metastatic spread. *ACS Nano*. 2015; 9: 733-45.
8. Kusumoto K, Akita H, Ishitsuka T, Matsumoto Y, Nomoto T, Furukawa R, et al. Lipid envelope-type nanoparticle incorporating a multifunctional peptide for systemic siRNA delivery to the pulmonary endothelium. *ACS Nano*. 2013; 7: 7534-41.
9. Wang WC, Cummings RD. The immobilized leucoagglutinin from the seeds of *Maackia amurensis* binds with high affinity to complex-type Asn-linked oligosaccharides containing terminal sialic acid-linked alpha-2,3 to penultimate galactose residues. *J Biol Chem*. 1988; 263: 4576-85.
10. Shibuya N, Goldstein IJ, Broekaert WF, Nsimba-Lubaki M, Peeters B, Peumans WJ. Fractionation of sialylated oligosaccharides, glycopeptides, and glycoproteins on immobilized elderberry (*Sambucus nigra* L.)

bark lectin. Arch Biochem Biophys. 1987; 254: 1-8.

11. Peters BP, Ebisu S, Goldstein IJ, Flashner M. Interaction of wheat germ agglutinin with sialic acid. Biochemistry. 1979; 18: 5505-11.

12. Ganguly P, Fossett NG. Role of surface sialic acid in the interaction of wheat germ agglutinin with human platelets. Biochem Biophys Res Commun. 1979; 89: 1154-60.

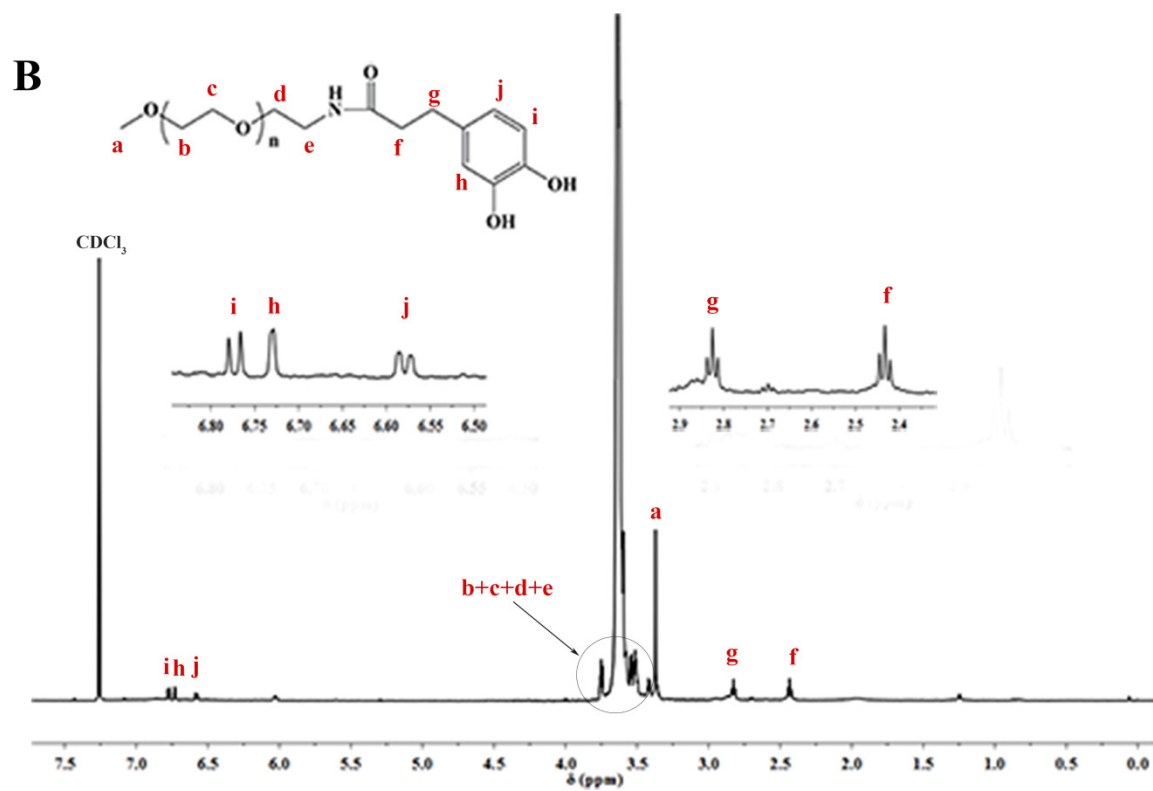
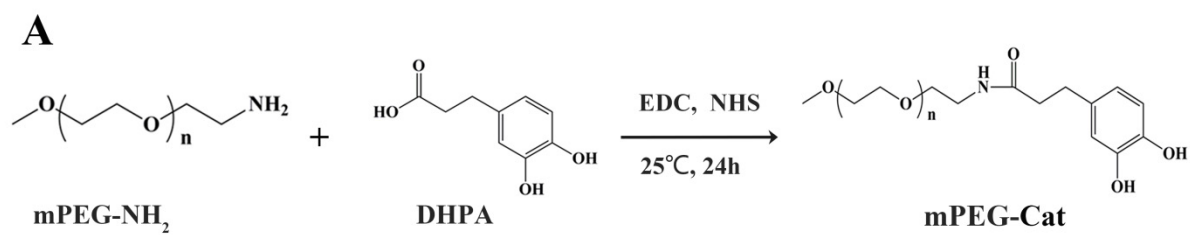


Figure S1. Synthesis of mPEG-Cat (A). ¹H NMR spectra of mPEG-Cat in CDCl₃ (B)

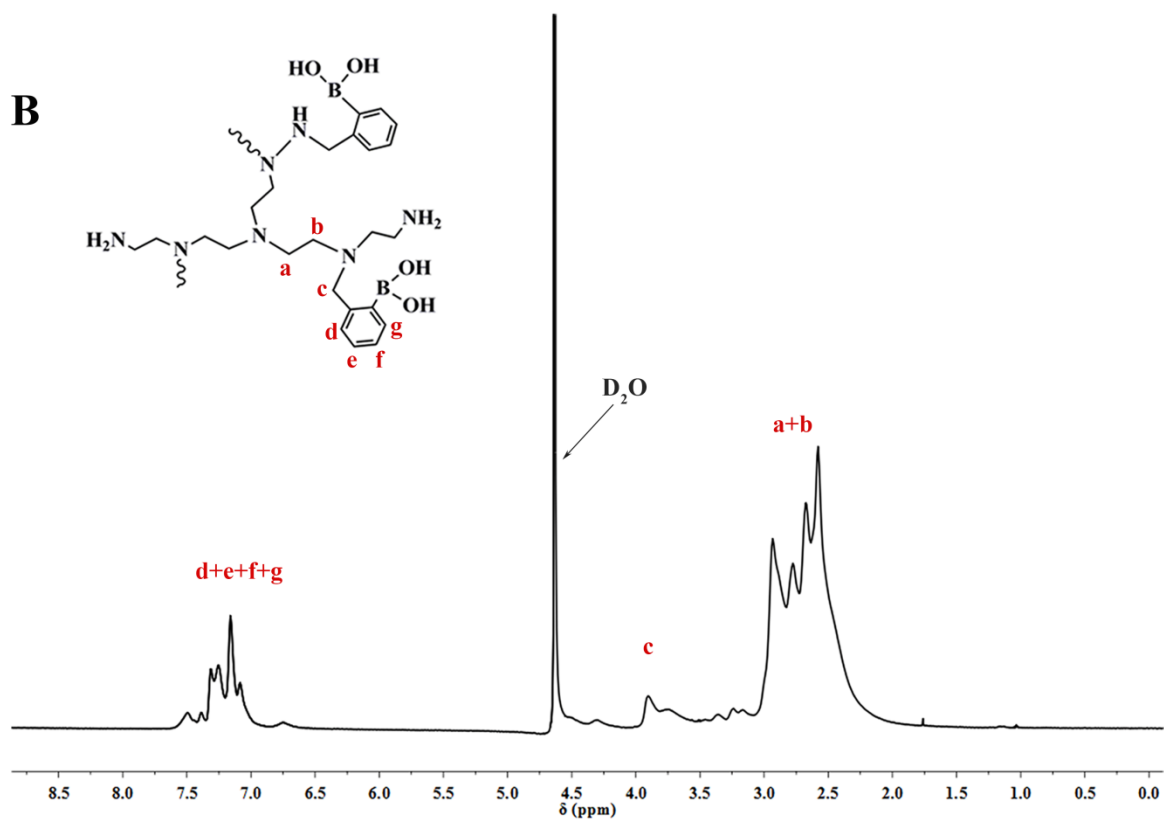
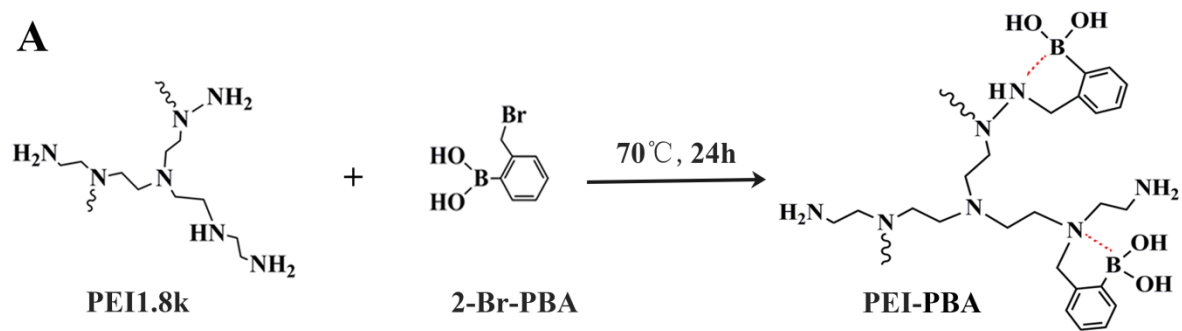


Figure S2. Synthesis of PEI-PBA (A). ¹H NMR spectra of PEI-PBA in D₂O (B)

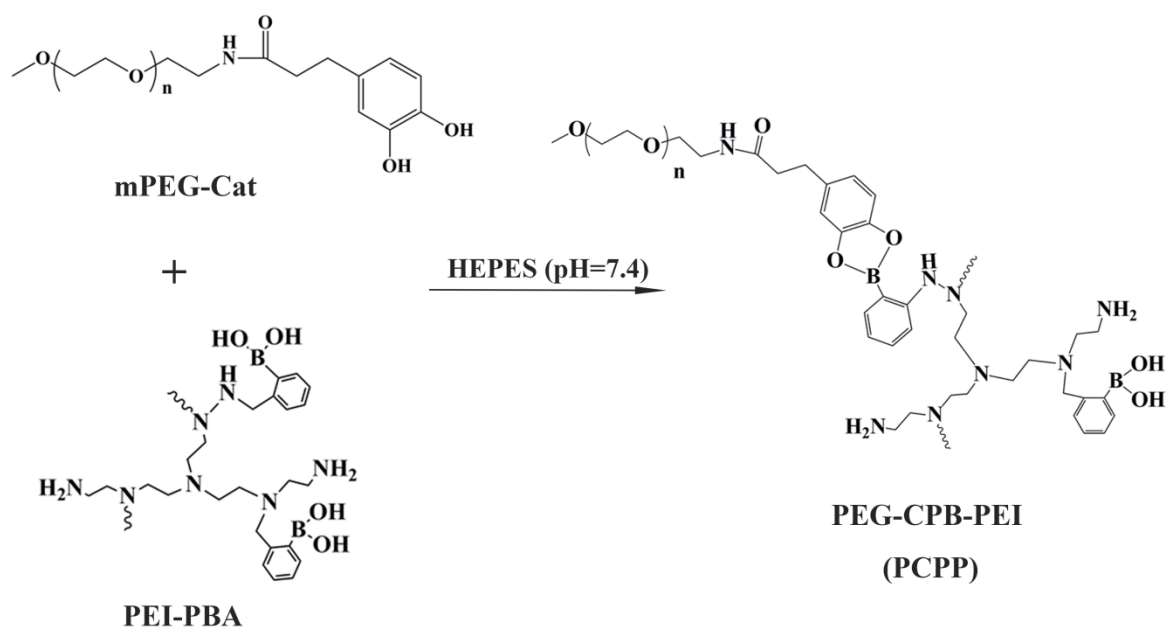


Figure S3. Synthesis of PCPP

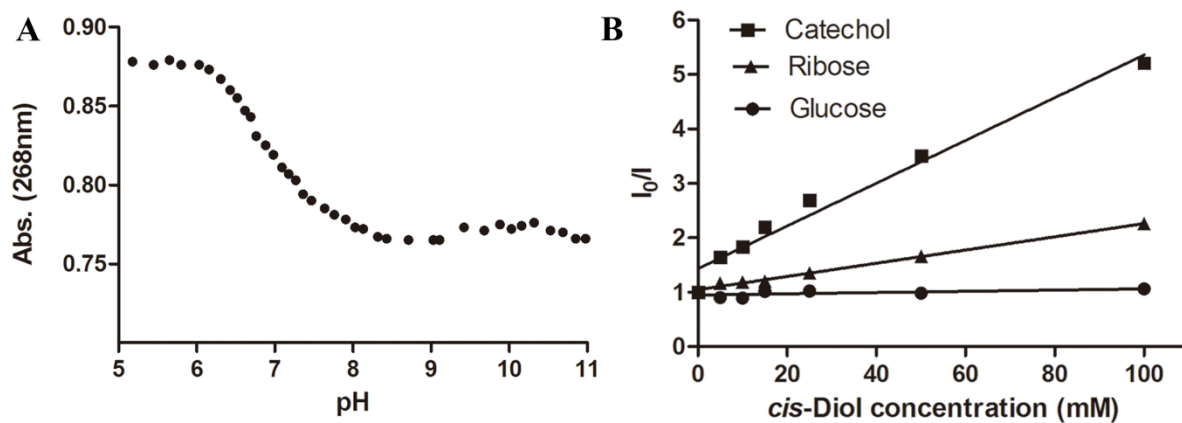


Figure S4. The pK_a determination of PEI-PBA by the absorbance change at 268 nm. PBA at 1.0 mM in 0.10 M phosphate buffer (A). The fluorescence of ARS/PEI-PBA in HEPES buffer at pH 7.4 was measured in the presence of catechol, ribose and glucose at various concentrations. I_0 and I represent the fluorescence intensity without and with *cis*-diol, respectively (B).

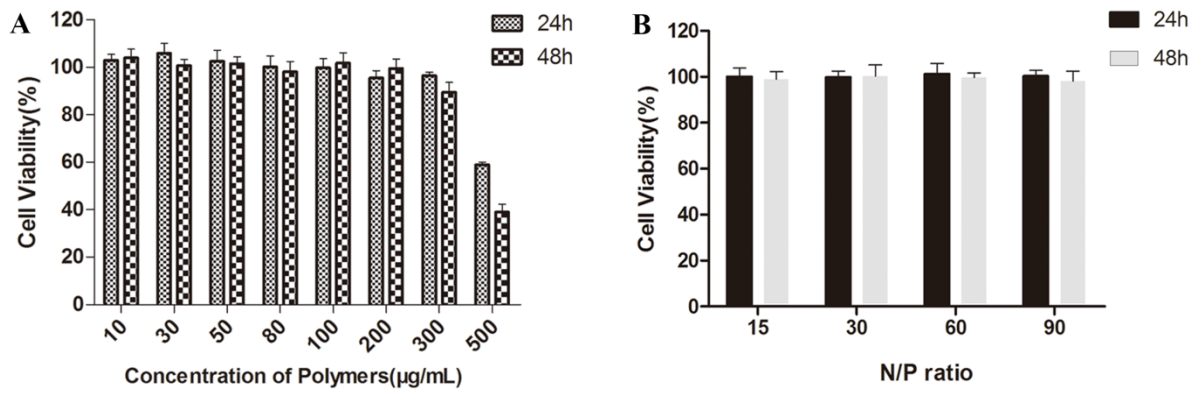


Figure S5. Cytotoxicity of PCPP with different concentrations (A) and PCPP_{siN.C.} nanoparticles at various N/P-ratios (B) on 4T1 cells for 24 or 48h (n=6).

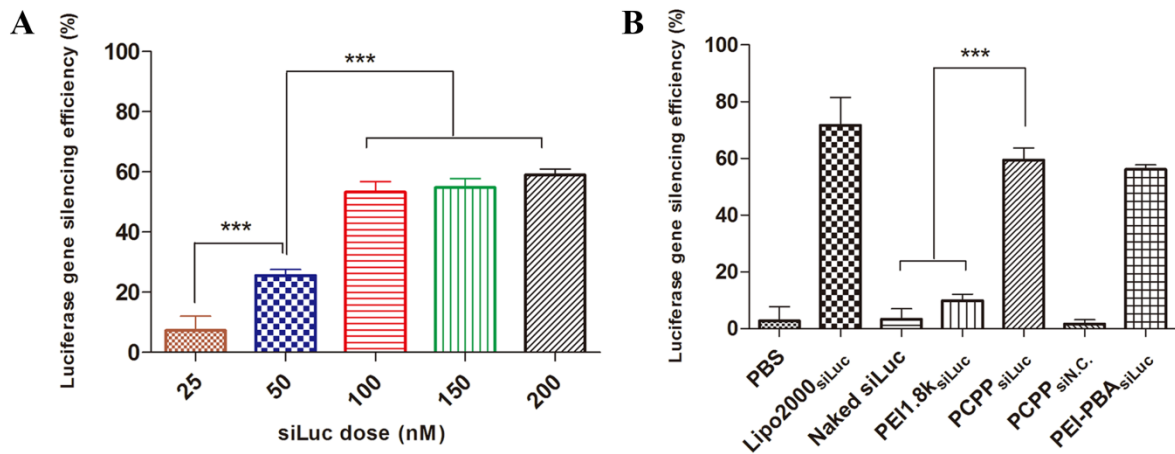


Figure S6. Luciferase gene silencing study of treatment with PCPP_{siLuc} at various doses (A) and different nanoparticles at the siLuc dose of 100 nM (B). (n = 3, *** $P < 0.001$).

